### DATA DRIVEN MODELLING OF PEEK MODULUS FOR ADVANCED PROCESS SIMULATION

Yannick T. Schäfer<sup>1</sup>, Kamyar Gordnian<sup>2</sup>, Ashley R. Chadwick<sup>1</sup>, Anoush Poursartip<sup>3</sup>

<sup>1</sup> German Aerospace Centre (DLR), Institute of Structures and Design Pfaffenwaldring 38-40, 70569 Stuttgart, Germany yannick.schaefer@dlr.de

<sup>2</sup> Convergent Manufacturing Technologies Inc.

<sup>3</sup> The University of British Columbia (UBC), Composites Research Network, Department of Materials Engineering

### **ABSTRACT**

The development of large-scale thermoplastic composite parts using conventional trial and error methods is prohibitively expensive due to the complex interaction of part geometry, layup and temperature history with residual stresses and subsequent deformation. Process simulation can be the key to making thermoplastic materials accessible, but is ultimately limited by the accuracy of the underlying material models. In this work, data fusion of mechanical and thermal test results is employed to correlate the modulus of neat PEEK to the crystallinity. Based on this database, a modulus model is developed as a function of the state variables of temperature and crystallinity.

#### 1. INTRODUCTION

Thermoplastic composite materials have been deployed for several decades, primarily in small scale structural components. Thermoplastics offer several advantages to thermoset matrix composites, including higher fracture toughness, good fatigue resistance and (re-)meltability allowing for welded integral designs, downstream reuse of material scraps and low-cost press forming [1]. Reduced manufacturing costs are expected due to the uncomplicated storage and high production rates associated with automated manufacturing technologies such as Automated Fibre Placement (AFP) [1, 2]. Among the applicable polymer types, poly-etherether-ketone (PEEK) is a widely used high-temperature matrix. For semi-crystalline thermoplastics such as PEEK, the viscoelastic behaviour and crystallization shrinkage lead to challenges with residual stresses and deformation upon demoulding, especially for complex thermal histories seen in AFP or 3D-printing [1, 2, 3]. High performance thermoplastic polymers drive the process and tooling costs due to the high melting temperatures and viscosity [4]. Process simulation aims to reduce the time and cost effort associated with the development of composite parts. The process and mould geometry can be optimized for improved mechanical performance and dimensional accuracy, as well as a reduction of process time. The accuracy of such model predictions is limited by the accuracy of the underlying material models. The behaviour of the composite material is influenced by the fibre and matrix properties, while the presence of fibres in turn alters the neat matrix properties. Deconvolution of polymer and fibre effects from tests on composites is difficult. Therefore, this work is focused on the stiffness properties of neat PEEK as a step towards the improvement of process simulation models based on experimental data.

#### 1.1 Stiffness Properties of PEEK

PEEK is a semi-crystalline polymer with a maximum crystallinity of 30-50% depending on the molecular weight [5]. It is characterized by a rigid glassy regime, followed by the glass transition around 150 °C where the amorphous regions undergo a second order phase change associated with a drop of the modulus. Above the glass transition is the rubbery regime, in which the crystallites remain rigid in a soft amorphous matrix. Amorphous PEEK can experience cold crystallization above  $T_g$ , but the main crystallization process occurs during cooling from the melt ( $T_m = 343$  °C).

The degree of crystallinity affects the mechanical properties of the polymer because crystalline structures exhibit a higher modulus. Ogale and McCullough reported data on the glassy state tensile modulus of PEEK as a function of crystallinity, showing an almost linear relation [6]. This effect can also be seen in other reported datasets [7, 8, 9, 10, 11]. Polymer science literature sometimes reports the glassy modulus to be constant [12, 13]. The effect of crystallinity in the rubbery regime is indeed larger in relative terms, as will be seen in the result section below or in literature reports [7], but the large absolute values in the glassy regime are not negligible for engineering applications. Additionally, higher degrees of crystallinity shift the glass transition to higher temperatures and leads to a broadening of the transition. This can be seen in reports of DMA tests in the literature [7, 8, 10] and is a result of reduced mobility of the polymer chains obstructed by adjacent crystalline structures.

Literature reports of the modulus of PEEK are usually given only as a function of temperature, and occasionally with the initial crystallinity [7, 14, 15, 16, 5]. The crystallinity is sometimes expressed as cooling rate or annealing temperature rather than crystallinity specifically [17, 10]. This is impractical for a modelling approach, especially because effects like cold crystallization cannot be addressed properly.

#### 1.2 Previous Modelling Approaches

To the authors knowledge, the only two comprehensive modelling approaches for PEEK were published by Chapman et al. [18] and Gordnian [19]. The latter is implemented in the COMPRO and RAVEN Common Component Architecture (CCA) framework by Convergent Manufacturing Technologies Inc. Lawrence et al. report another model, but the underlying equations are not published explicitly, and the datasets appears to be limited to  $200\,^{\circ}$ C [10]. Although the characteristics of PEEK have been studied for several decades, the knowledge is scattered and the quantitative data necessary for accurate engineering models is particularly rare in the temperature regime above the glass transition temperature  $T_g$  and up to the melting point  $T_m$ . The named modelling approaches are based on a mix of experimental data, assumptions, and simplifications. Chapman modelled the glassy regime as a function of crystallinity but constant with respect to temperature. Both glass transition and rubbery regime are modelled with simple linear function. Gordnian, following the polymer physics assumption, modelled the glassy regime as constant and invariant with crystallinity, but provides a sophisticated transition shape.

The aim of this research is to generate experimental data of PEEK tensile modulus as a function of temperature and crystallinity over a wide range of temperatures covering the processing range. A model of the dynamic modulus is derived and reported with all constitutive equations.

#### 2. RESEARCH TESTS & EXPERIMENTS

#### 2.1 Materials

The tests were conducted with VICTREX PEEK 600G, which was acquired in 1 and 2 mm plates produced from Ensinger Inc. (*TECAPEEK® CAL*). The use of manufactured plates reduces errors from enclosed porosity but required a stress relief annealing step to avoid deformation from residual stresses upon heating close to melt. Crystallinity was varied by cooling from the melt in varying cooling rates or to different isothermal temperatures (in the rheometer), or by varying the initial crystallinity (for DMA). Varying degrees of crystallinity were achieved by annealing and quenching plates of material. The plates were placed on a 1 mm aluminium shim to carry the melt. The material was quenched with the shim in room temperature water. Figure 1 shows the temperature cycle and material after heat treatment.

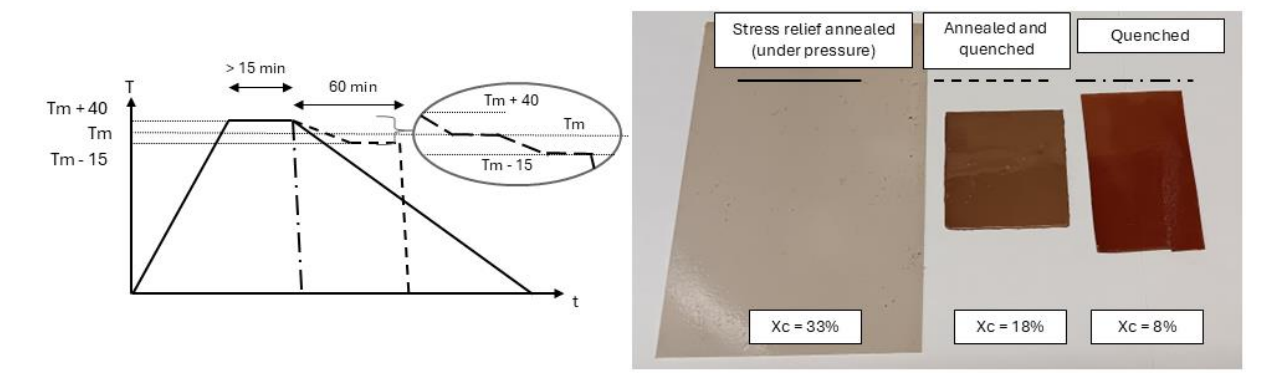


Figure 1: Annealing cycle (left) and resulting sample material colour (right)

### 2.2 Differential Scanning Calorimetry (DSC)

DSC tests were used to determine the state of crystallinity and to trace the crystallization process for the specific temperature histories used in mechanical tests. A TA Instruments DSC 2000 was used with aluminium Tzero pans and hermetic lids. Sample masses were in the order of 10 mg. For tests cooling from the melt, the crystallinity was calculated from the crystallization enthalpy. The melting peak was used for DMA tests, where the samples were heated from the glassy state. If cold crystallization occurred, the cold crystallization peak was subtracted from the melting peak. The calculation is based on equation (1) and uses a reference heat of fusion of 130 J/g [20]. The peaks are integrated in steps of 1 °C to track the crystallization kinetics in a custom python tool. Cubic Hermite polynomials are used as baselines with tangential transition to the DSC curve. The mean result of three repeats was used for correlation.

$$X_{mc} = \frac{|H_m| - |H_c|}{\Delta H_{ref}} \tag{1}$$

### 2.3 Rheometry

Rheometry tests were conducted on a TA Instruments HR-3 Discovery Hybrid Rheometer with 8 mm (for crystallization) and 25 mm (for melt region analysis) parallel plates with the TRIOS software. A temperature lag compensation was derived from separate runs with 8 mm plates of each cooling rate with an embedded thermocouple. Nitrogen purge gas was used to prevent oxidation during melting. The samples were heated to the holding temperature (360 °C) and

the gap was fixed. Excess material was cut off to ensure accurate geometry. The temperature cycle is depicted in figure 2. All tests were conducted at a frequency of 1 Hz and a strain of 0.1 %, which is well within the linear viscoelastic range determined by strain sweeps.

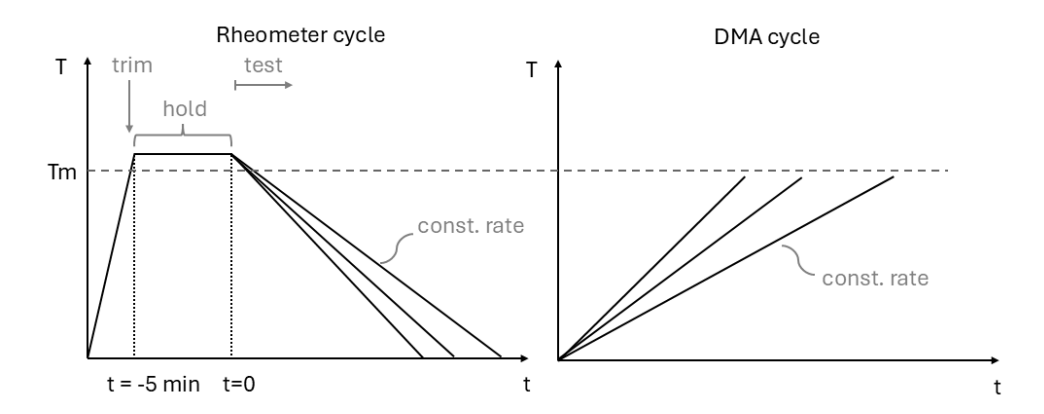


Figure 2: Rheometer and DMA temperature cycle

### 2.4 Dynamic Mechanical Analysis (DMA)

DMA tests were performed in 3-point bending mode with 50 mm support spacing on a TA Discovery DMA 850. The beam cross section was approximately 10 x 1 mm to achieve a tensile dominated behaviour. A temperature lag compensation was derived from separate test runs with a thermocouple applied to the surface. A Force-Track of 125 % was used to always ensure contact with the sample. The tests were conducted at 1 Hz and 0.1 % strain for the fully crystalline beams, and 0.05 % strain for the lower crystallinity beams to reduce creep.

#### 2.5 Data Processing

The mechanical and DSC tests were designed with similar temperature histories to allow correlation of the crystallinity state at each instant. Because temperature changes drive the crystallization more than time, correlation was done in temperature space to reduce the uncertainty.

### 2.6 Modelling Approach

It is convenient for modelling purposes to consider semi-crystalline PEEK to be a composite material of crystallites in an amorphous matrix. The interaction of the constituents is expected to follow a lower-bound (Reuss) type relation due to the surrounding matrix. Here, the Mori-Tanaka model for particle reinforcements is applied (as reviewed in [21]).

The glass transition is an exclusively amorphous phenomenon, while melting is a phenomenon exclusive to the crystallites [12]. Here, the decrease of crystalline modulus is assumed to be linear with temperature. This effect is adapted from reports for metallic single crystals [22] and somewhat linear results for ultradrawn polyethylene [23]. DMA data reported in the literature [7, 17, 10] confirms this assumption, although it is sometimes obstructed by logarithmic scaling. The amorphous modulus is assumed to also behave linearly based on the rubber elasticity theory, where  $E = 3\rho RT/M_n$  [12] combined with linear changes in density under a constant coefficient of thermal expansion. To summarize, the constituent crystalline and amorphous moduli are modelled as continuous, and discontinuous linear equations through  $T_g$ , respectively. Furthermore, the crystalline function is assumed to be continuous above  $T_m$ ,

therefore attributing the drop of modulus around melt to the decrease of crystallinity rather than a decrease of the crystalline modulus. For simplicity, the effect of crystalline morphology is neglected in this work. While it is difficult to measure the amorphous modulus above  $T_g$ , due to crystallization and the low modulus, it is easy to measure the shear modulus of the amorphous melt in a rheometer. The experimental melt modulus is implemented as a high temperature limit of the model. The transformation into the tensile modulus is done with equation (2) assuming isotropic properties and a Poisson's ratio of  $\nu = 0.5$ .

$$E = G \cdot 2(1 + \nu) = 3G \tag{2}$$

The glass transition, driven by mobility of the polymer chains [12], is affected by the degree of crystallinity. Increasing crystallinity inhibits mobility and shifts the transition to higher temperature and leads to a widening of the transition. This can be observed in the DMA results in the literature [7, 8, 10]. The transition is therefore modelled as a sigmoidal function, in which  $T_g$  and the width of the transition are linear functions of the degree of crystallinity, and which is scaled with temperature to fit the shape of the transition well.

The final model equations are achieved by fitting the underlying equations to the DMA data for high and low initial crystallinity. The medium crystallinity run remains as a control dataset. The fit is then adjusted to fit the rheometer data close to the melting temperature.

#### 3. RESULTS

#### 3.1 Experimental Data

Figure 3 displays the crystallinity data for the three initial conditions at 5 cpm heating rate (left diagram). The low and medium crystallinity samples (initial values 8 and 18 %m) exhibit a distinct cold-crystallization peak above  $T_{\rm g}$  (exotherm pointing up), which is not present in the fully crystalline state of 33 %m. Upon cooling from the melt, the onset of crystallization and peak rate temperature shift down with increasing cooling rate (right diagram). In temperature space, the peak area appears larger for higher rates because the time span between two temperatures is smaller.

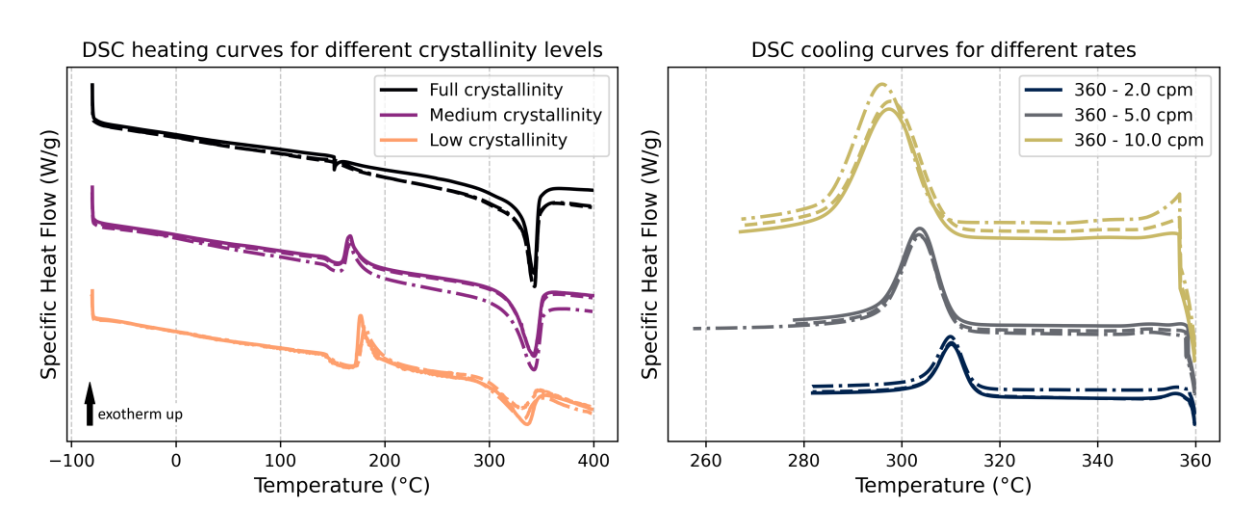


Figure 3: DSC heat flow diagram for the three initial degrees of crystallinity (left) and at different cooling rates from the melt

Figure 4 displays the melt region shear modulus for low cooling rates from 380 °C. The datapoints agree well throughout the applied rates and is approximately linear. Figure 5 shows the modulus change with temperature and correlated crystallinity. The data shows a strong increase of modulus with the onset of crystallization, and a reduction of gradient once crystallization is completed (below 290...310 °C). In this region, the temperature change drives the increase of modulus, which manifests as a steep incline in crystallinity space (right image). The shift of crystallization temperatures matches the DSC curves, which then leads to a similar behaviour of all cooling rates in crystallinity space.

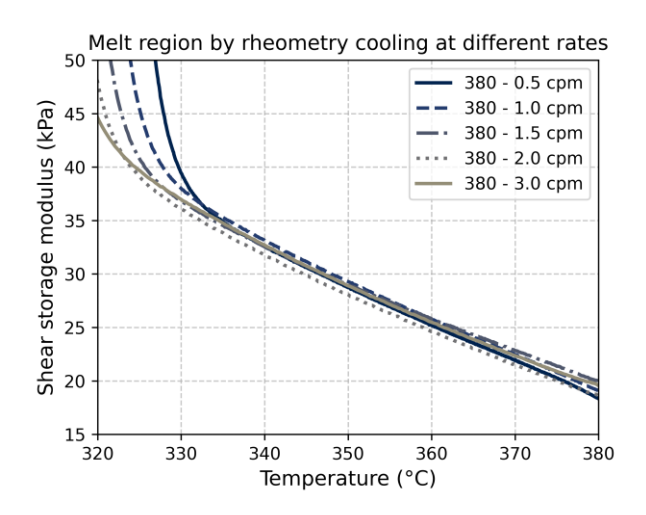


Figure 4: Melt shear modulus from 25 mm plate rheometry

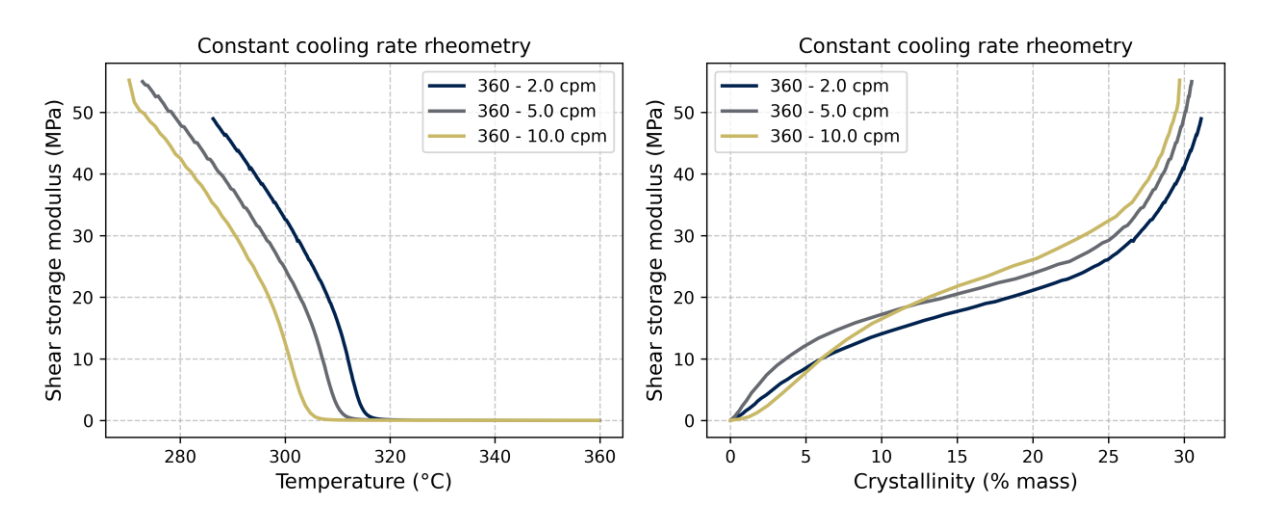


Figure 5: Shear modulus at constant cooling rates with temperature correction

Figure 6 shows the DMA results for the initial crystallinities at constant heating rates. The glass transition is shifted to higher temperatures for the fully crystalline samples and the transition is wider. The medium crystallinity sample experiences cold crystallization, associated with an increase in modulus from approx. 180 °C. The low crystallinity sample collapses under its own weight around  $T_{\rm g}$  due to the low modulus, at which point the test fails.

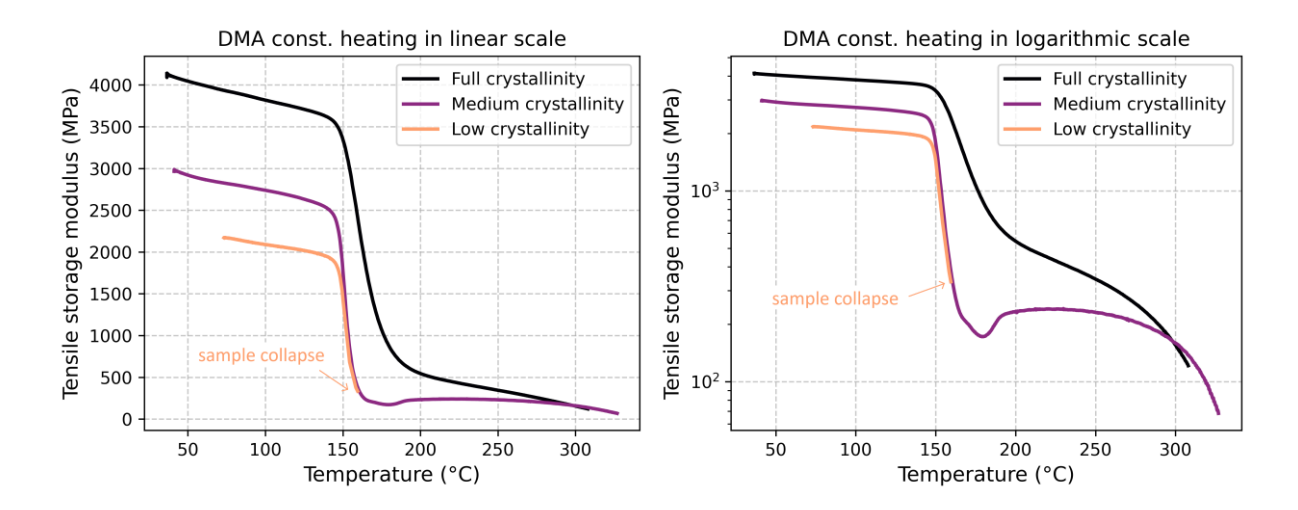


Figure 6: DMA heating curves for different initial crystallinities in lin. and log scale

#### 3.2 Model Equations

The constituent moduli functions are as follows in the units of MPa and °C, where the indices a and c denote the amorphous and crystalline fractions, respectively.

$$E_c = 14643.71 - 10.20 \cdot T \tag{3}$$

$$E_{a,alassy} = 1884.80 - 2.66 \cdot T \tag{4}$$

$$E_{a,rubbery} = max \begin{cases} 79.37 - 0.2319 \cdot T \text{ (below melt)} \\ 0.441687 - 0.001014 \cdot T \text{ (above melt)} \end{cases}$$
 (5)

The crystal volume fraction is defined as

$$X_{vc} = X_c = \frac{X_{mc}}{X_{mc} + \frac{\rho_c}{\rho_a} (1 - X_{mc})}$$
 (6)

The transition is modelled with the sigmoidal mixing function M, scaled with temperature and crystallinity to fit the data.

$$T_{g,mid} = 150 + 8 \cdot \frac{X_c}{0.35}, \qquad \Delta T_{T_g} = 5 + 15 \cdot \frac{X_c}{0.35}, \qquad T_{g,onset} = T_{g,mid} - \Delta T_{T_g}$$
 (7)

$$S_{T_g} = \begin{cases} 1 + 0.8 & \frac{T - T_{g,onset}}{2 \Delta T_{T_g}} & \text{if } T > T_{g,onset} \\ 1 & \text{otherwise} \end{cases}$$
(8)

$$\overline{\Delta T_{Tg}} = S_{T_g} \cdot \Delta T_{T_g} \tag{9}$$

$$M(T) = \left(1 + \exp\left(6 \cdot \frac{T - T_{g,mid}}{\overline{\Delta T_{T_g}}}\right)\right)^{-1}$$
(10)

$$E_a = E_{a,rubbery} + \left(E_{a,glassy} - E_{a,rubbery}\right) \cdot M(T) \tag{11}$$

The interaction is based on the Mori-Tanaka model (adapted from [21]), where the index m denotes the combined matrix properties, and K and G are the bulk and shear moduli. The Poisson's ratios are assumed to be  $v_a = v_c = 0.38 = const.$ 

$$K_a = \frac{E_a}{3(1 - 2\nu_a)}, \qquad K_c = \frac{E_c}{3(1 - 2\nu_c)}, \qquad G_a = \frac{E_a}{2(1 + \nu_a)}, \qquad G_c = \frac{E_c}{2(1 + \nu_c)}$$
 (12)

$$f_a = \frac{G_a(9 K_a + 8 G_a)}{6(K_a + 2 G_a)} \tag{13}$$

$$K_m = K_a + \frac{X_c(K_c - K_a)}{1 + (1 - X_c) \left[ \frac{3(K_c - K_a)}{3K_a + 4G_a} \right]}, \qquad G_m = G_a + \frac{X_c(G_c - G_a)}{1 + (1 - X_c) \left[ \frac{G_c - G_a}{G_c + f_a} \right]}$$
(14)

$$E_m = \frac{9 \, K_m G_m}{3 \, K_m + G_m} \tag{15}$$

Figure 7 displays the glass transition mixing function M(T) (left) and the constituent moduli in linear and logarithmic scaling. The crystalline modulus is lower than previously reported in the literature. Ogale and McCullough [6] reported 30 GPa, and the mean of the orthotropic moduli reported by Pisani et al. [24] and Kashmari et al. [11] is around 50 GPa, assuming an averaging effect from the spherulitic morphology. This deviation is a result of the assumed Mori-Tanaka relationship and may change with different micromechanical models.

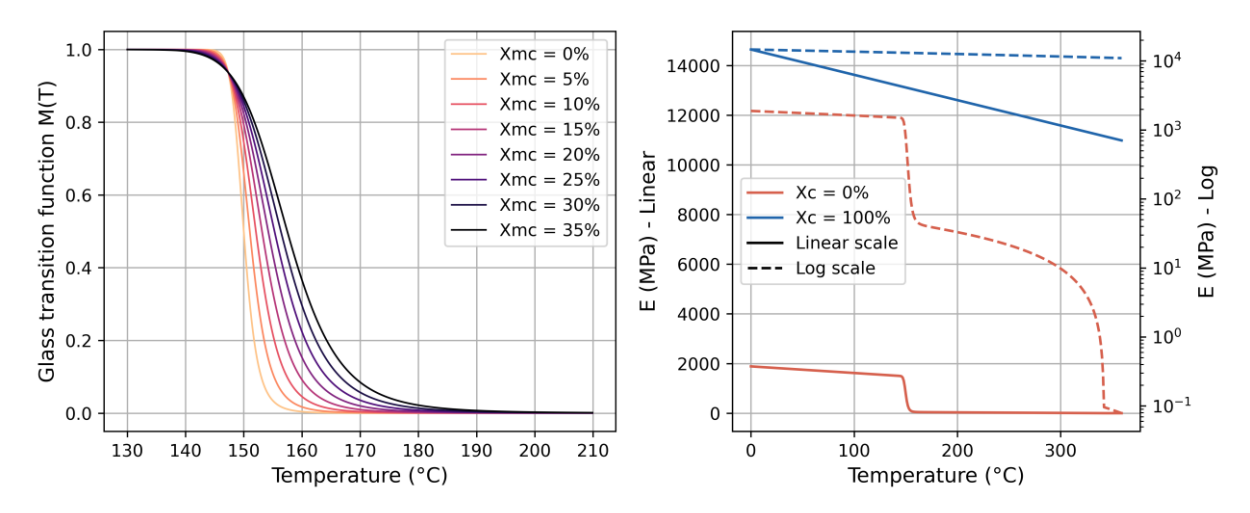
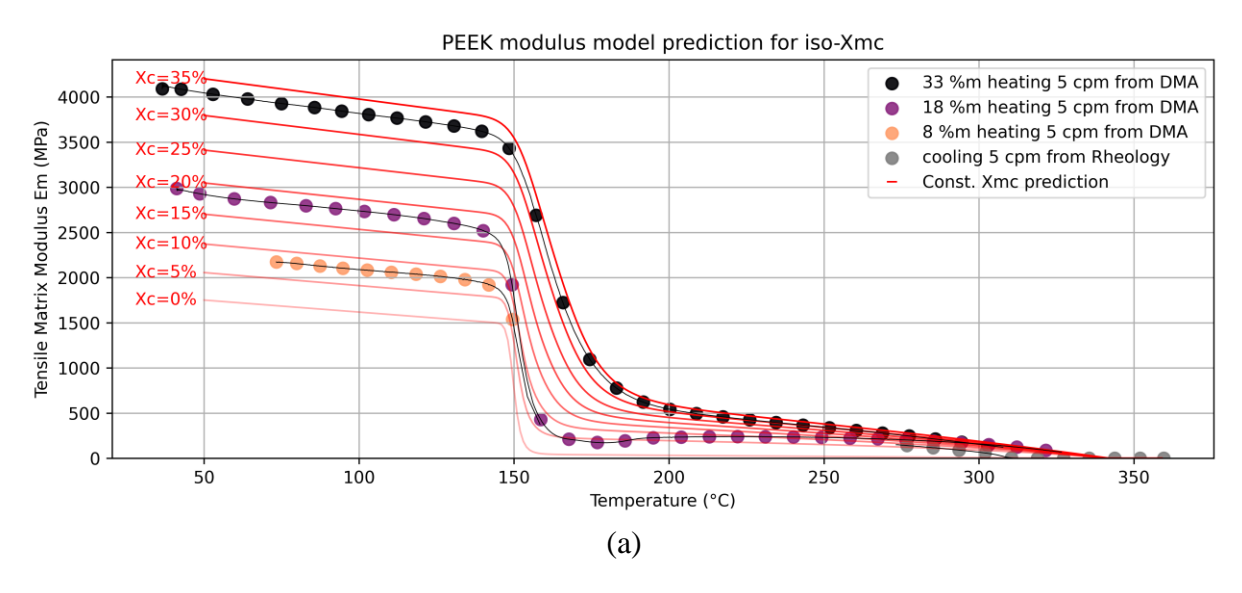
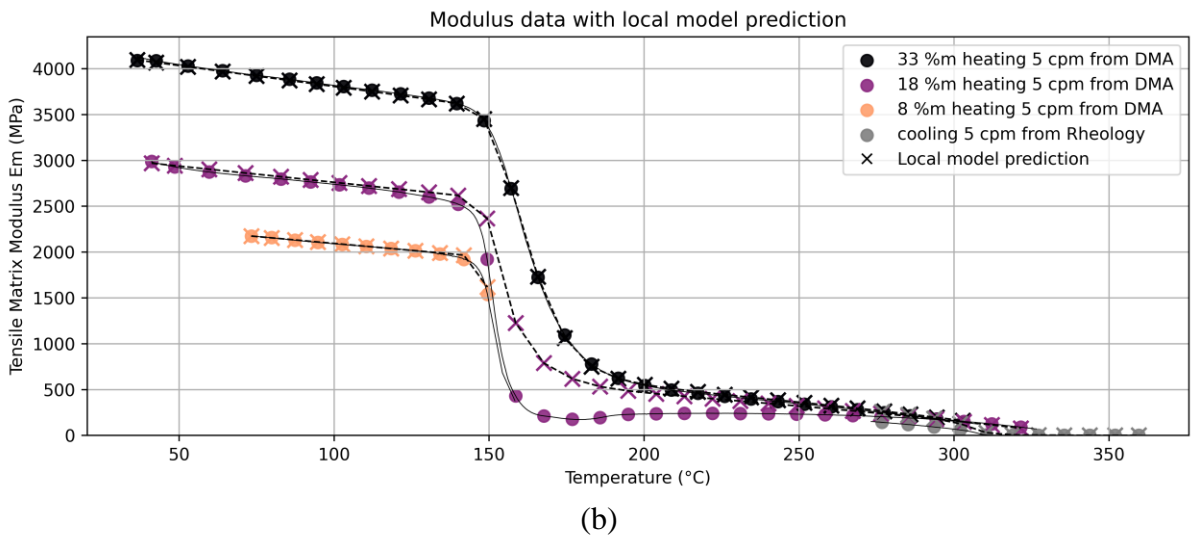


Figure 7: Glass transition function (left) and tensile modulus of the constituents (right)

### 3.3 Model Prediction and Comparison to Experimental Data

The model prediction is displayed in figure 8, showing the envelope of the modulus as isocrystallinity lines (a), and a local prediction based on the experimental dataset of temperature and crystallinity (b). The graph (c) shows both prediction types focused on the rubbery and melt regime. The glassy regime appears linear due to the relatively similar modulus of the constituents. In this regime, the prediction is accurate. The glass transition shape is matched well, especially for the full crystallinity data. In the rubbery regime, the high crystallinity curve is fitted well, but the medium crystallinity modulus is overpredicted by the model. This is due to the use of the Mori-Tanaka model in all regimes, which appears to be not accurate when the amorphous modulus becomes very low. The morphology of the crystallites may also be partly responsible, as the assumption of particle reinforcement becomes inaccurate if the spherulites impinge on each other at full crystallinity. The rheometry data does not exactly match the DMA data (8c). This is likely due to the assumption of a Poisson's ratio of 0.38 for the conversion of G to E, and a general inaccuracy of modulus measurements in the rheometer and DMA.





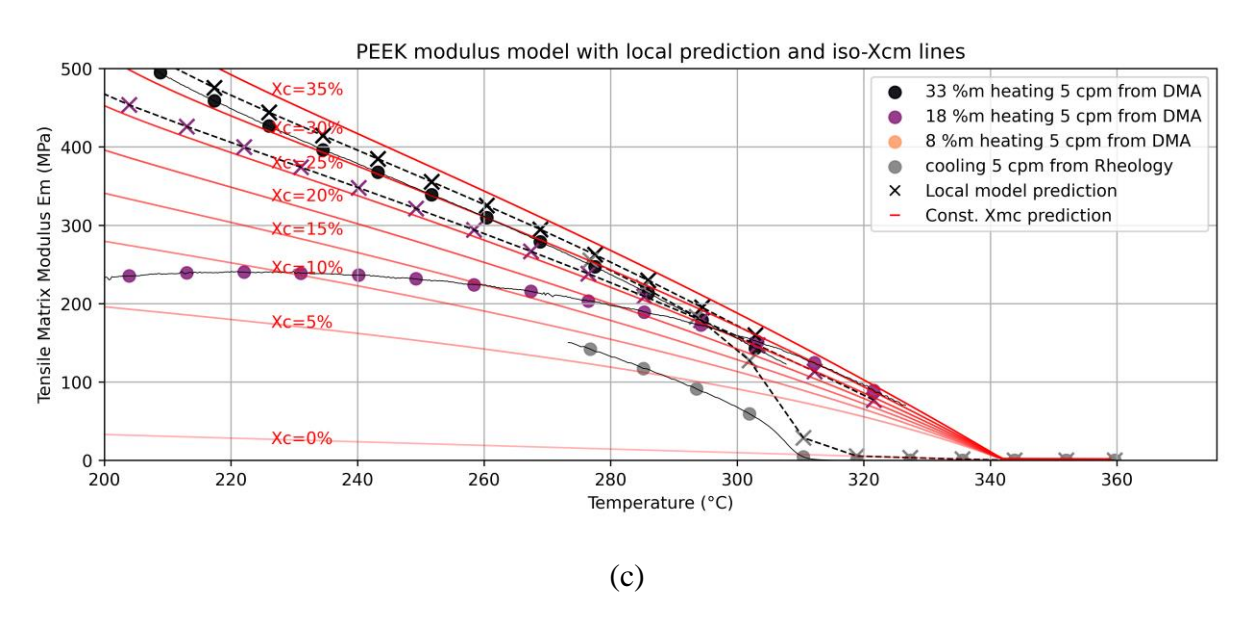


Figure 8: Model prediction in temperature space for const. crystallinity (a), local crystallinity (b), and zoomed to the rubbery and melt regime (c)

### 4. CONCLUSIONS

This paper has presented a methodology to correlate the state of crystallinity to the mechanical properties of polymers by means of DSC, DMA and rheometer tests. The method was applied to neat PEEK samples of varying initial crystallinity, achieving a unique dataset over the entire processing temperature range. From the experimental data, a model of the dynamic modulus of PEEK was derived and presented in detail. The underlying assumed functional relation of the constituent moduli is linear with temperature and continuous (crystallites), and discontinuous (amorphous) through the glass transition. The glass transition is modelled as a sigmoid function, which is adjusted with the degree of crystallinity and temperature to fit the experimental data. The Mori-Tanaka model for particle reinforced composites is used to model the interaction of crystalline and amorphous parts.

The model prediction is overall good in the glassy regime, and throughout the glass transition and rubbery regime for full crystallinity. The data driven modelling as a function of both state variables temperature and crystallinity in all temperature regimes is a key improvement to previous modelling approaches. The medium crystallinity modulus above  $T_{\rm g}$  is overpredicted due to the functional relation in the Mori-Tanaka model.

Future work should focus on the relaxation properties of the viscoelastic, thermo-rheologic complex behaviour of PEEK to expand the model into the time space. The methodology should be applied to other applied polymer systems (such as low-melt-polyaryletherketone) and composite materials to validate the method and investigate the influence and interaction of fibre reinforcements on the modulus.

In the next step, this model will be implemented and subsequently validated by means of spring-in prediction for coupons and elements.

#### 5. REFERENCES

- [1] R. Krueger and A. Bergan, "Advances in Thermoplastic Composites Over Three Decades—A Literature Review," NASA STI Program Report Series; National Aeronautics and Space Administration: Washington, DC, USA, 2024.
- [2] S. Nowotny, G. Doll, A. Chadwick, P. Dreher and D. Fricke, "The potential of Insitu Laser-AFP for thermoplastic composites for high performance structures," in 5th Workshop on structural analysis of lightweight structures, 2018.
- [3] D. Fricke, L. Raps and I. Schiel, "Prediction of warping in thermoplastic AFP-manufactured laminates through simulation and experimentation," *Advanced Manufacturing: Polymer & Composites Science*, vol. 8, p. 1–10, 2022.
- [4] S. Pantelakis and K. Tserpes, Revolutionizing aircraft materials and processes, Springer, 2020.
- [5] K. L. White, L. Jin, N. Ferrer, M. Wong, T. Bremner and H.-J. Sue, "Rheological and thermal behaviors of commercial poly (aryletherketone) s," *Polymer Engineering & Science*, vol. 53, p. 651–661, 2013.
- [6] A. A. Ogale and R. L. McCullough, "Influence of microstructure on elastic and viscoelastic properties of polyether ether ketone," *Composites science and technology*, vol. 30, p. 185–201, 1987.
- [7] A. D'Amore, A. Pompo and L. Nicolais, "Viscoelastic effects in poly (ether ether ketone)(PEEK) and PEEK-based composites," *Composites science and technology*, vol. 41, no. 3, pp. 303--325, 1991.
- [8] Z. Wu, Y. B. Zheng, Z. Ni, T. Nakamura and R. Yosomiya, "Effect of thermal history on the crystallization behaviour of polyetheretherketone by the dynamic viscoelastometer," *Die Angewandte Makromolekulare Chemie: Applied Macromolecular Chemistry and Physics*, vol. 164, p. 103–113, 1988.
- [9] W. J. Unger and J. S. Hansen, "The effect of cooling rate and annealing on residual stress development in graphite fibre reinforced PEEK laminates," *Journal of Composite Materials*, vol. 27, p. 108–137, 1993.
- [10] W. E. Lawrence, J. C. Seferis and J. W. Gillespie Jr, "Material response of a semicrystalline thermoplastic polymer and composite in relation to process cooling history," *Polymer composites*, vol. 13, p. 86–96, 1992.
- [11] K. Kashmari, H. Al Mahmud, S. U. Patil, W. A. Pisani, P. Deshpande, M. Maiaru and G. M. Odegard, "Multiscale process modeling of semicrystalline PEEK for tailored thermomechanical properties," *ACS applied engineering materials*, vol. 1, p. 3167–3177, 2023.
- [12] J. M. G. Cowie and V. Arrighi, Polymers: chemistry and physics of modern materials, CRC press, 2007.
- [13] L. H. Sperling, Introduction to physical polymer science, John Wiley & Sons, 2005.
- [14] M. Yuan, J. A. Galloway, R. J. Hoffman and S. Bhatt, "Influence of molecular weight on rheological, thermal, and mechanical properties of PEEK," *Polymer Engineering & Science*, vol. 51, p. 94–102, 2011.
- [15] C.-c. M. Ma, H.-c. Hsia, W.-l. Liu and J.-t. Hu, "Thermal and rheological properties of poly (phenylene sulfide) and poly (ether etherketone) resins and composites," *Polymer composites*, vol. 8, p. 256–264, 1987.

- [16] J. R. Sarasua and J. Pouyet, "Dynamic mechanical behavior and interphase adhesion of thermoplastic (PEEK, PES) short fiber composites," *Journal of Thermoplastic Composite Materials*, vol. 11, p. 2–21, 1998.
- [17] R. K. Krishnaswamy and D. S. Kalika, "Dynamic mechanical relaxation properties of poly(ether ether ketone)," *Polymer*, vol. 35, pp. 1157-1165, 1994.
- [18] T. J. Chapman, J. W. Gillespie Jr, R. B. Pipes, J.-A. E. Manson and J. C. Seferis, "Prediction of process-induced residual stresses in thermoplastic composites," *Journal of composite materials*, vol. 24, p. 616–643, 1990.
- [19] K. Gordnian, Crystallization and thermo-viscoelastic modelling of polymer composites, PhD Thesis, 2017.
- [20] C. N. Velisaris and J. C. Seferis, "Crystallization kinetics of polyetheretherketone (peek) matrices," *Polymer Engineering & Science*, vol. 26, p. 1574–1581, 1986.
- [21] S. Zhao, Z. Zhao, Z. Yang, L. Ke, S. Kitipornchai and J. Yang, "Functionally graded graphene reinforced composite structures: A review," *Engineering Structures*, vol. 210, p. 110339, 2020.
- [22] H. Zeng, Z. Zhang, M. Zhang, J. Xu, N. Jian and K. Mai, "Young's modulus of transcrystallinities in semicrystalline thermoplastic composites," *Journal of applied polymer science*, vol. 54, p. 541–551, 1994.
- [23] M. Matsuo and C. Sawatari, "Temperature dependence of the crystal lattice modulus and the Young's modulus of polyethylene," *Macromolecules*, vol. 21, p. 1653–1658, 1988.
- [24] W. A. Pisani, M. S. Radue, S. Chinkanjanarot, B. A. Bednarcyk, E. J. Pineda, K. Waters, R. Pandey, J. A. King and G. M. Odegard, "Multiscale modeling of PEEK using reactive molecular dynamics modeling and micromechanics," *Polymer*, vol. 163, p. 96–105, 2019.